IEEE Access
Multidisciplinary | Rapid Review | Open Access Journal

Received October 22, 2018, accepted November 18, 2018, date of publication November 30, 2018,
date of current version December 27, 2018.

*Digital Object Identifier 10.1109/ACCESS.2018.2884245*

# Statistical Linearization Analysis of a Hydropneumatic Suspension System With Nonlinearity

**ZUTI ZHANG, SHUPING CAO, AND CHUNHONG RUAN**
School of Mechanical Science and Engineering, Huazhong University of Science and Technology, Wuhan 430074, China
Corresponding author: Chunhong Ruan (ruanch_2018@163.com)

This work was supported in part by the China Postdoctoral Science Foundation under Grant 2018M632834 and in part by the Fundamental Research Funds for Central Universities under Grant HUST JCTD2016202.

**ABSTRACT** Hydropneumatic suspension has the characteristics of nonlinear stiffness, nonlinear friction damping, and nonlinear hydraulic damping, and therefore, it has been widely applied to heavy vehicles. A hydropneumatic suspension with a special structure was proposed and studied in this paper. The nonlinear quarter-vehicle model was built by using Newton's laws according to its configuration. Then, this nonlinear mathematic model was linearized through the statistical linearization method on the basis of random vibration theory. Next, the transfer functions of the suspension system subjected to random road excitation were built according to the statistical linearization model and the power density spectrum approach. In addition, the responses of vehicle body acceleration, tire relative dynamic load, and suspension deflection with respect to the wideband random excitation due to road roughness were obtained according to the James formula. Next, the influences of the equivalent damping ratio and the equivalent frequency ratio on vehicle riding comfort, riding safety, handing stability, and suspension reliability were analyzed through simulations. These results provided the basic principles for selecting the reasonable hydropneumatic suspension parameters.

**INDEX TERMS** Statistical linearization, nonlinearity, hydropneumatic suspension.

## I. INTRODUCTION

A suspension system is a crucial component for determining a heavy vehicle's dynamic performances, and it is responsible for riding comfort, riding safety, handling stability and vehicle suspension reliability. Riding comfort is evaluated by the level of vehicle body acceleration, and it is usually related to the ability of the vehicle to isolate passengers from the uncomfortable vibrations arising because of irregular road excitation. Riding safety is normally evaluated by the tire relative dynamic load. Handling stability is achieved by guiding the vehicle along the track. The vehicle needs to maintain good contact between its tires and the road, so the tire deflection amplitude is the determinant index to evaluate its performance [1]–[2]. Suspension reliability is associated with the suspension stoke, which should be protected against collisions, and suspension deflection is usually the evaluation criteria. Because its nonlinear nature can provide higher mobility and increase riding comfort, hydropneumatic suspension has been widely used in heavy vehicles [3]–[8]. In theory, the compressibility of gas in the hydropneumatic suspension makes it resilient and provides a soft spring stiffness at lower wheel travel and a hard spring stiffness at higher wheel travel. Therefore, it has stiffness nonlinearity. At the same time, the existence of an orifice gives it hydraulic damping nonlinearity. Narayanan and Senthil [9] and Narayanan and Raju [10] built a 2 Degree of Freedom (2-DOF) quarter-vehicle model that has the characteristics of nonlinear velocity, quadratic damping and hysteretic stiffness. A modified Boucs model was utilized to describe the hysteretic feature of the suspension spring [11]. Verros *et al*. [12] studied the characteristics of damping and stiffness excited by random road disturbance by use of nonlinear quarter-car models and presented an optimization method.

As an input excitation term, road surfaces feature is a significant parameter while analyzing the suspension performance. Generally, assuming that typical road surfaces are 2-dimensional Gaussian random processes with the characteristics of homogenization and isotropy makes it possible to use a single power spectral density to completely model a road profile [13], [14]. In addition, nonlinear algebraic

equations can be yielded in the forms of the response of second-order moments and their time-derivatives through the spectral density approach [15]. Thompson *et al.* [16] used spectral decomposition methods to study a half-vehicle model with a preview controller excited by random road disturbance. Turkay and Akcay *et al.* [17] used a reasonably low-order rational function to describe a typical road surface in terms of power spectrum and analyzed the root-mean square random responses of the vehicle system with respect to the road excitation with white/colored noise velocity. Wu and Law [18] assumed that the responses of a vehicle system and the random road surface are Gaussian random processes. Furthermore, the random road disturbance is simplified as stochastic inputs [9].

The hydropneumatic suspension system simplified as an MDOF nonlinear vibration system with wide band random excitation can be suitably analyzed using a statistical linearization method [3], [15], [19]. The equivalent linearization technique has been widely applied to analyze the nonlinear systems subjected to random excitations [20]–[22]. Atalik and Utku [15] yielded the response of a nonlinear MDOF dynamic system to stationary Gaussian excitations by using an equivalent linearization technique. Dong and Luo [19] researched the dynamic response of a hydropneumatic suspension using statistical linearization based on the 2-DOF nonlinear suspension model. The nonlinear stiffness of the hydropneumatic spring was replaced with its first three terms Taylor series at the static equilibrium position, and the responses were analyzed using numerical simulation. Jin and Luo [3] studied the stochastic random response of a half vehicle model running on a rough road, and the model has the nonlinear characteristics of hysteretic stiffness and square damping. The output of a first-order linear filter to Gaussian white noise was used to model the road roughness height, and the statistics response of the nonlinear suspension was determined by using the equivalent linearization method. Gopala Rao and Narayanan [23], [24] studied the stationary random response of a nonlinear passive vehicle suspension running on a homogenous rough road. The Bouc-Wen model was used to describe the hysteretic nonlinearity of suspension, and an equivalent linear model was derived by use of a statistical linearization technique.

Few studies comprehensively analyze the effects of suspension parameters on riding comfort, handing stability and riding safety. The suspension parameters are generally designed empirically and lack theoretical guidance. In this study, on the basis of the design of a hydropneumatic spring, a quarter-vehicle model with nonlinear stiffness, nonlinear friction damping and nonlinear hydraulic damping characteristics was built by using Newton's laws. This nonlinear mathematical model was linearized by use of a statistical linearization method on the basis of random vibration theory. The nonlinear stiffness of the hydropneumatic spring was replaced with the first two terms of its Taylor series at the static equilibrium position and further linearized by using an equivalent linearization technique. The nonlinear friction damping and nonlinear hydraulic damping were also linearized. Furthermore, the transfer functions of the suspension system subjected to the random excitation were built using the statistical linearization model and power spectrum density approach. Then, the responses of the vehicle body acceleration, tire relative dynamic load, and suspension deflection subjected to the wide band random excitations caused by road roughness were obtained by use of the James Formula. Finally, the equivalent damping ratio and equivalent frequency ratio were defined, and their influences on vehicle riding comfort, riding safety, handing stability and suspension reliability were analyzed through simulations.

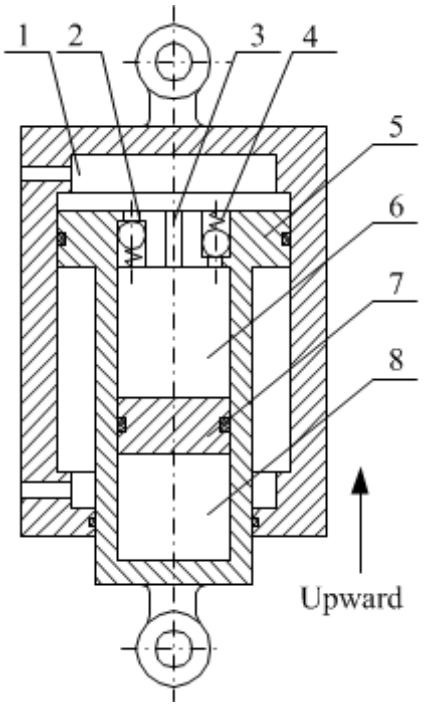


**FIGURE 1.** Diagram of Hydropneumatic suspension: 1-outer oil chamber, 2-compression check valve, 3-fixed orifice, 4-extension check valve, 5-main piston, 6-inner oil chamber, 7-floating piston, 8-gas chamber.

## II. SUSPENSION CONFIGURATION

A hydropneumatic spring was proposed and its general configuration is as shown in **Figure 1**. This hydropneumatic spring mainly consists of an outer oil chamber, 4 compression check valves, a fixed orifice, 4 extension check valves, a main piston, an inner oil chamber, a floating piston and a gas chamber, and other components. The chamber within the main piston is divided into a gas chamber and an inner oil chamber, and the closed volume of nitrogen gas is separated from the inner oil chamber containing the working medium by means of the floating piston. The inner oil chamber communicates with the outer oil chamber through the fixed orifice. The 4 compression check valves and 4 extension check valves are arranged around the orifice at equal intervals. When the external load increases, the distance between the vehicle body and chassis decreases, and the working medium pressure in

the outer oil chamber rises to open the compression check valves. Consequently, the working medium flows into the inner oil chamber through the fixed orifice and the compression check valves, and further compresses the gas by displacing the floating piston. The shrinkage of the gas chamber makes the gas pressure increase, and the force exerted on the main piston ultimately reaches dynamic balance with the external load. However, if the external load on the suspension reduces, the process is reversed as gas expansion forces the floating piston to move upwards because of the high pressure nitrogen gas. Simultaneously, the working medium flows back to the outer oil chamber through the fixed orifice and extension check valves. As a result, the distance between the vehicle body and the chassis increases, and the force acting on the main piston decreases accordingly. Ultimately, it reaches a dynamic balance state. In the working process of the hydropneumatic spring, the compression and expansion of the gas chamber gives it spring-like features, and its basic function for isolating vibration is realized. In addition, its stiffness is variable owing to the compressibility of nitrogen. Meanwhile, it has hydraulic damping nonlinearity because of the existence of a hydraulic orifice. These special characteristics make it possible to improve the riding comfort, riding safety, handing stability and suspension reliability. In general, the special structure gives this hydrosuspension some additional characteristics:

The gas chamber is designed within the main piston, so it has the advantages of good sealing performance, compact structure, small size and light weight.

In comparison with diaphragm structure, the separation of oil and gas by means of the floating piston makes the hydrosuspension have longer strokes, and the volume of the gas chamber can be adjusted conveniently according to the demands of stiffness.

The fixed orifice can be optimized according to the characteristics of the vehicle.

The vehicle height can be adjusted by charging or discharging oil in the outer oil chamber to adapt to various road environments and vehicle characteristics.

## III. NONLINEAR SUSPENSION MODEL

**Figure 2** shows the quarter-vehicle suspension model, which was built on the basis of the structure feature of the hydropneumatic suspension. Here, $m_1$ represents the unsprung mass, $m_2$ is the sprung mass. $k_t$ denotes the tire stiffness coefficient, which is simplified as a constant. $A_c$ is the orifice cross area. $A$ is the equivalent cross-area of the main piston. $p_0$ and $V_0$ are the pressure and volume of nitrogen at the initial equilibrium position. $p_1$ and $V_1$ are the instantaneous dynamic pressure and volume of nitrogen gas. $p$ is the pressure of working medium in the outer oil chamber. $z_r$ is the disturbance excitation due to irregular road surfaces, $z_u$ is the displacement of unsprung mass, and $z_s$ is the displacement of sprung mass. $F_f$ is the friction force.

According to the physical model of the suspension system and Newton's second law, the theoretical model is described

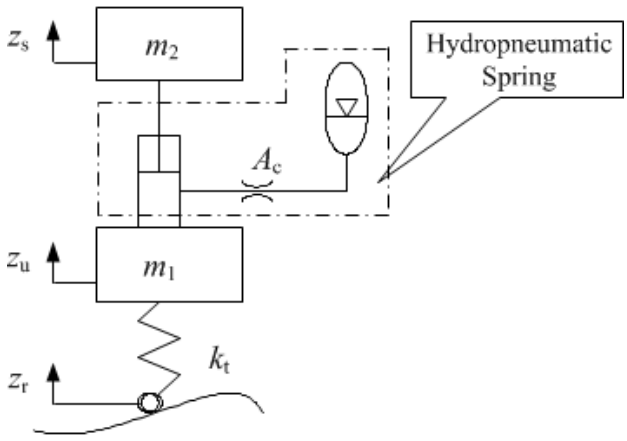


**FIGURE 2.** Schematic diagram of a quarter-vehicle suspension system.

by two coupled nonlinear differential equations:

$$\begin{cases} m_1\ddot{z}_u = k_t(z_r - z_u) - pA + p_0A - F_f\text{sign}(\dot{z}_u - \dot{z}_s) \\ m_2\ddot{z}_s = pA - p_0A + F_f\text{sign}(\dot{z}_u - \dot{z}_s) \end{cases} \tag{1}$$

The flow rate passing through the orifice can be expressed as:

$$A(\dot{z}_u - \dot{z}_s) = C_dA_c\sqrt{\frac{2}{\rho}|p - p_1|}\text{sign}(\dot{z}_u - \dot{z}_s) \tag{2}$$

where $C_d$ is the flow coefficient, and $C_d = 0.65$; $\rho$ is working medium density.

Assuming the nitrogen gas enclosed in the gas chamber follows the adiabatic compression and expansion processes, the following formula can be given according to the gas state equation:

$$p_1V^{1.4} = p_0V_0^{1.4} \tag{3}$$

The volume of nitrogen can be further expressed as:

$$V = V_0 - A(z_u - z_s) \tag{4}$$

Consequently, the suspension system can be modeled as:

$$\begin{cases} m_1\ddot{z}_u = k_t(z_r - z_u) - m_2\ddot{z}_s \\ m_2\ddot{z}_s - \left[\left(\dfrac{V_0}{V_0 - A(z_u - z_s)}\right)^{1.4} - 1\right]p_0A \\ \quad = \left[R(\dot{z}_u - \dot{z}_s)^2 + F_f\right]sign(\dot{z}_u - \dot{z}_s) \end{cases} \tag{5}$$

where $R$ is the hydraulic damping coefficient, and $R = \left(\frac{A}{C_dA_c}\right)^2\frac{\rho A}{2}$. Defining the tire deflection $z_1 = z_r - z_u$ and the suspension deflection $z_2 = z_u - z_s$, Eq. (5) can be further rewritten as:

$$\begin{cases} (m_1 + m_2)\ddot{z}_1 + m_2\ddot{z}_2 + k_tz_1 - (m_1 + m_2)\ddot{z}_r = 0 \\ m_2(\ddot{z}_1 + \ddot{z}_2 - \ddot{z}_r) + F_k + R\dot{z}_2^2\text{sign}(\dot{z}_2) + F_f\text{sign}(\dot{z}_2) = 0 \end{cases} \tag{6}$$

where $F_k = \left[\left(\frac{V_0}{V_0 - Az_2}\right)^{1.4} - 1\right]p_0A = \left[\left(\frac{V_0}{V_0 - Az_2}\right)^{1.4} - 1\right]m_2g$, which is the suspension elastic force associated with the suspension deflection ($z_2$).

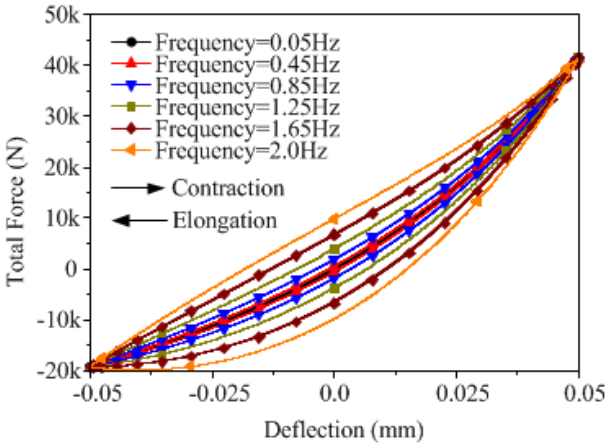


**FIGURE 3.** The total force of hydropneumatic suspension subjected to deflection.

The total force exerted on the hydropneumatic suspension is shown in **Figure 3**. It has obvious hysteresis characteristics. The total force would increase with the increase of deflection amplitude. Under the same deflection conditions, the force during the contraction process is much higher than that during the elongation process because of the variable characteristic of stiffness. Simultaneously, the total force is also affected by the deflection frequency. The higher the deflection frequency is, the stronger are the hysteresis and the nonlinear characteristics.

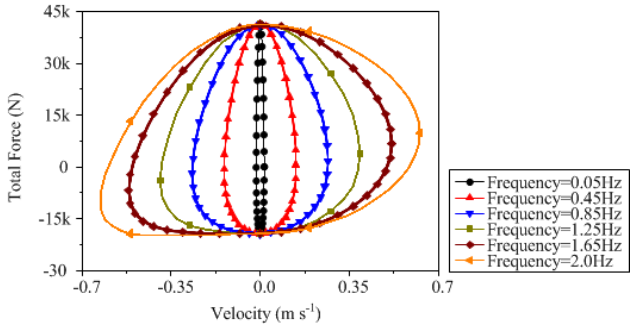


**FIGURE 4.** The total force of hydropneumatic suspension subjected to velocity.

**Figure 4** shows the relationship between the total force and deflection velocity. The higher deflection velocity means a higher deflection frequency and would lead to stronger hysteresis. In other words, reducing the deflection frequency and velocity is an effective method to decrease the nonlinearity.

The deflection velocity and frequency would dramatically affect the nonlinearity of hydropneumatic suspension as discussed above. In fact, they mainly influence the damping force. As shown in **Figure 5** and **Figure 6**, damping force is an important nonlinear item. The higher deflection frequency would have a higher maximum deflection velocity, and the maximum damping force would be accordingly higher. The damping force would quadratically increase with the increase of deflection velocity.

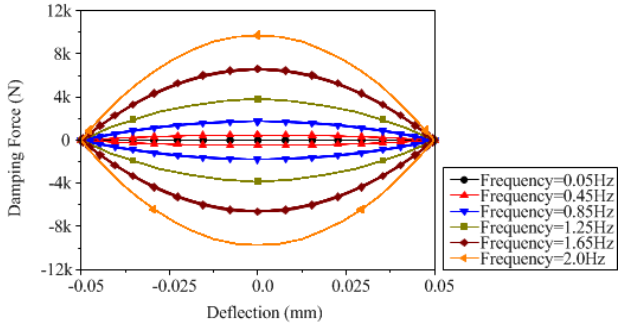


**FIGURE 5.** The damping force of hydropneumatic suspension subjected to deflection.

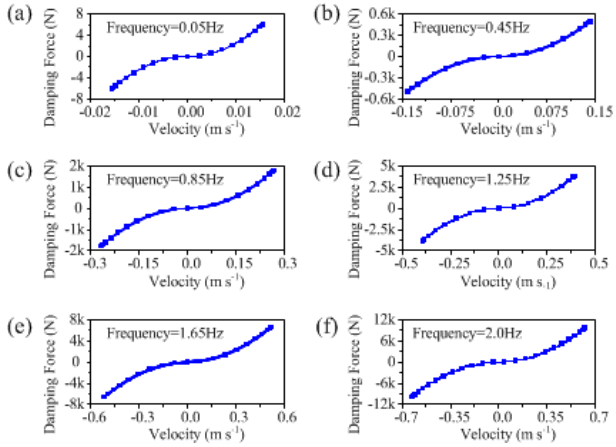


**FIGURE 6.** Damping force of hydropneumatic suspension subjected to velocity.

The stiffness variation is another nonlinear item. Because the stiffness during the contraction process is higher than that during the elongation process, the elastic force is much higher during the contraction process. The elastic force would nonlinearly increase with the increase in deflection, as shown in **Figure 7**. Friction force is another nonlinear item. In this study, the sample Coulomb model was used to describe the friction force. It is considered a constant and its direction is opposite to the direction of motion.

## IV. LINEARIZATION

As analyzed in section 3, the mathematical model of the hydropneumatic suspension has the characteristics of nonlinear hydraulic damping, nonlinear stiffness and nonlinear friction damping, and it is excited by road roughness, which can be assumed to be a wide band random process. It is reasonable to apply the statistical linearization method to linearize the nonlinear model [3], [15], [19]. The nonlinear model can be linearized by replacing the nonlinear terms with linear equations, and the coefficients of the linear equations could be obtained through minimizing the mean-square errors between the linear and nonlinear equations.

The nonlinear square hydraulic damping term $F(\dot{z}_2) = R\dot{z}_2^2 \mathrm{sign}(\dot{z}_2)$ is equivalent to $F_*(\dot{z}_{2*}) = \lambda_1 + \lambda_2 \dot{z}_{2*}$, where $\dot{z}_{2*} = \dot{z}_2 - m_{\dot{z}_2}$, $m_{\dot{z}_2}$ is the mean value of $\dot{z}_2$.

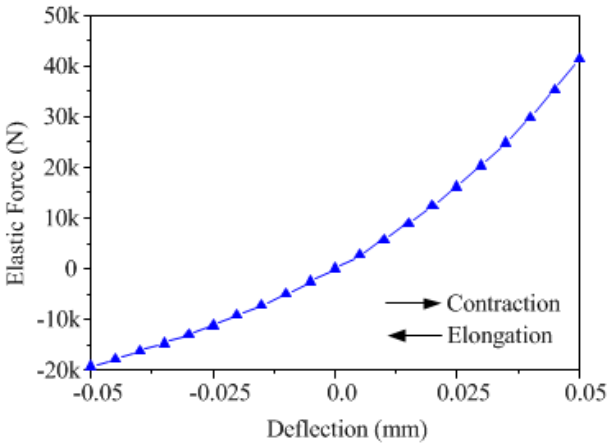


**FIGURE 7.** The elastic force of hydropneumatic suspension subjected to displacement.

The suspension deflection is assumed to be a stationary stochastic process [16], so its time derivative is equal to zero, i.e., $m_{\dot{z}_2} = 0$ and $\dot{z}_{2*} = \dot{z}_2$. The logical choice of coefficients $\lambda_1$ and $\lambda_2$ is to minimize the mean-square error, and the mean-square error is given by:

$$E\left[\Delta F^2\right] = \int_{-\infty}^{\infty} \left[F\left(\dot{z}_2\right) - \lambda_1 - \lambda_2 \dot{z}_{2*}\right]^2 p\left(\dot{z}_2\right) \mathrm{d}\dot{z}_2 \quad (7)$$

Supposing the vehicle body velocity $(\dot{z}_2)$ is a stationary Gaussian stochastic process [18], the probability density function of $\dot{z}_2$ can be expressed as $p\left(\dot{z}_2\right) = \frac{1}{\sqrt{2\pi}\sigma_{\dot{z}_2}} \exp\left(-\frac{\dot{z}_2^2}{2\sigma_{\dot{z}_2}^2}\right)$, where $\sigma_{\dot{z}_2}^2$ is the variance value of $\dot{z}_2$. Using a minimum of $E\left[\Delta F^2\right]$ as the criteria, i.e., the first partial derivatives with respect to $\lambda_1$ and $\lambda_2$ are zero, the following expressions can be obtained:

$$\begin{cases} \lambda_1 = \int_{-\infty}^{\infty} F\left(\dot{z}_2\right) p\left(\dot{z}_2\right) \mathrm{d}\dot{z}_2 \\ \lambda_2 = \frac{1}{\sigma_{\dot{z}_2}^2} \int_{-\infty}^{\infty} F\left(\dot{z}_2\right) \dot{z}_2 p\left(\dot{z}_2\right) \mathrm{d}\dot{z}_2 \end{cases} \quad (8)$$

Substituting $F\left(\dot{z}_2\right)$ and $p\left(\dot{z}_2\right)$ into Eq. (8), the solutions of $\lambda_1$ and $\lambda_2$ are derived as: $\lambda_1 = 0$, $\lambda_2 = \frac{4R}{\sqrt{2\pi}}\sigma_{\dot{z}_2}$

In addition, the friction force makes the hydropneumatic suspension possess a nonlinear hysteresis characteristic, and its physical characteristic is similar to damping. Thus, it can be simplified and linearized by use of equivalent linearization technique:

$$F_{\mathrm{f}} \mathrm{sign}(\dot{z}_2) = \lambda_3 \dot{z}_2 \quad (9)$$

where $\lambda_3$ is the equivalent linear friction coefficient. For a stationary stochastic process, the average power of the equivalent linear friction damping in a large interval [0, T] can be expressed as:

$$w_1 = \frac{1}{T} \int_0^T \lambda_3 \dot{z}_2^2 \mathrm{d}t \quad (10)$$

Considering the mean value of $\dot{z}_2$ is zero, i.e., $m_{\dot{z}_2} = 0$, the average power can be further described as:

$$w_1 = \lambda_3 \sigma_{\dot{z}_2}^2 \quad (11)$$

For a stationary stochastic process, the average power of a constant friction force in a large enough interval [0, T] can also be expressed as:

$$w_2 = F_{\mathrm{f}} \frac{1}{T} \int_0^T |\dot{z}_2| \, \mathrm{d}t \quad (12)$$

where $\frac{1}{T}\int_0^T |\dot{z}_2| \, \mathrm{d}t$ is the first-order absolute moment of the suspension deflection velocity $(\dot{z}_2)$, and $\dot{z}_2$ is a stationary Gaussian stochastic process [18]. Then, we have:

$$\frac{1}{T} \int_0^T |\dot{z}_2| \, \mathrm{d}t = 0.798 \sigma_{\dot{z}_2} \quad (13)$$

According to the energy conservation principle $(w_1 = w_2)$, that is,

$$\lambda_3 \sigma_{\dot{z}_2}^2 = 0.798 \sigma_{\dot{z}_2} F_{\mathrm{f}} \quad (14)$$

The equivalent linear friction damping coefficient can yield:

$$\lambda_3 = \frac{0.798 F_{\mathrm{f}}}{\sigma_{\dot{z}_2}} \quad (15)$$

Considering the comprehensive influence of friction damping and hydraulic orifice damping, the total equivalent damping coefficient is given by:

$$\lambda = \lambda_2 + \lambda_3 \quad (16)$$

Meanwhile, the elastic force can be simplified through Taylor series expansion at the equilibrium position, and this equilibrium position is set as the coordinate origin:

$$F_{\mathrm{k}}\left(z_2\right) = k_1 \Delta z_2 + k_2 \left(\Delta z_2\right)^2 + k_3 \left(\Delta z_2\right)^3 + \cdots \quad (17)$$

where $k_1 = \frac{1.4 m_2 g A}{V_0}$, $k_2 = \frac{1.68 m_2 g A^2}{V_0^2}$ and $k_3 = \frac{1.9 m_2 g A^3}{V_0^3}$, choosing the first two terms, and the Taylor series expansion is based on the coordinate origin, that is, $\Delta z_2 = z_2$ , so the elastic force of hydropneumatic can be further simplified as:

$$F_{\mathrm{k}}\left(z_2\right) = k_1 z_2 + k_2 z_2^2 \quad (18)$$

Then, the simplified nonlinear elastic force is replaced with the linear equation $F_{\mathrm{k}*}\left(z_{2*}\right) = k_0 + k z_{2*}$, where $z_{2*} = z_2 - m_{z2}$, $\dot{z}_2$ is the mean value of $z_2$, $k_0$ and $k$ are selected to minimize the mean-square error, and the mean-square error can be given by:

$$E\left[\Delta F_{\mathrm{k}}^2\right] = \int_{-\infty}^{\infty} \left[F_{\mathrm{k}}\left(z_2\right) - k_0 - k z_{2*}\right]^2 p_{\mathrm{k}}\left(z_2\right) \mathrm{d}z_2 \quad (19)$$

Supposing the suspension deflection $(z_2)$ follows Gaussian distribution, and its probability density function can be expressed as: $p_{\mathrm{k}}\left(z_2\right) = \frac{1}{\sqrt{2\pi}\sigma_{z_2}} \exp\left(-\frac{(z_2 - m_{z_2})^2}{2\sigma_{z_2}^2}\right)$, $\sigma_{z_2}^2$ is the variance value of $z_2$. As a minimization criterion on $E\left[\Delta F_{\mathrm{k}}^2\right]$, the first partial derivatives with respect to $k_0$ and $k$ should

be zero. Simultaneously, substituting $F_{\mathrm{k}}(z_2)$ and $p_{\mathrm{k}}(z_2)$ into Eq. (19), the following results can be obtained:

$$\begin{cases} k_0 = k_1 m_{z_2} + k_2\left(\sigma_{z_2}^2 + m_{z_2}^2\right) \\ k = k_1 + 2k_2 m_{z_2} \end{cases} \tag{20}$$

Thus, the nonlinear model, i.e., Eq. (6) is rewritten as:

$$\begin{cases} (m_1+m_2)\ddot{z}_1 + m_2\ddot{z}_2 + k_{\mathrm{t}} z_1 - (m_1+m_2)\ddot{z}_{\mathrm{r}} = 0 \\ m_2\left(\ddot{z}_1 + \ddot{z}_2 - \ddot{z}_{\mathrm{r}}\right) + k(z_2 - m_{z_2}) + \lambda\dot{z}_2 + k_0 = 0 \end{cases} \tag{21}$$

Supposing $z_1$, $z_2$ and $z_{\mathrm{r}}$ follow stationary stochastic processes, i.e., the time derivative of each expected value vanishes [25]. By computing the mathematical expectation on both sides of Eq. (21), the mean value of $z_1$ and $k_0$ can be derived ($m_{z1} = 0$, $k_0 = 0$). Combining with Eq. (20), these results are given by:

$$\begin{cases} m_{z_2} = \dfrac{k - k_1}{2k_2} \\ k = \sqrt{k_1^2 - 4k_2^2\sigma_{z_2}^2} \end{cases} \tag{22}$$

After central processing, the mathematical model of the hydropneumatic suspension can be further rewritten as:

$$\begin{cases} (m_1+m_2)\ddot{z}_{1*} + m_2\ddot{z}_{2*} + k_{\mathrm{t}} z_{1*} - (m_1+m_2)\ddot{z}_{\mathrm{r}*} = 0 \\ m_2\left(\ddot{z}_{1*} + \ddot{z}_{2*} - \ddot{z}_{\mathrm{r}*}\right) + kz_{2*} + \lambda\dot{z}_{2*} = 0 \end{cases} \tag{23}$$

Substituting $z_{1*} = z_{\mathrm{r}*} - z_{\mathrm{u}*}$ and $z_{2*} = z_{\mathrm{u}*} - z_{\mathrm{s}*}$ into Eq. (23), the statistical linearization model is given by:

$$\begin{cases} m_1\ddot{z}_{\mathrm{u}*} + \lambda\left(\dot{z}_{\mathrm{u}*} - \dot{z}_{\mathrm{s}*}\right) + k_{\mathrm{t}} z_{\mathrm{u}*} + k\left(z_{\mathrm{u}*} - z_{\mathrm{s}*}\right) = k_{\mathrm{t}} z_{\mathrm{r}*} \\ m_2\ddot{z}_{\mathrm{s}*} - \lambda\left(\dot{z}_{\mathrm{u}*} - \dot{z}_{\mathrm{s}*}\right) - k\left(z_{\mathrm{u}*} - z_{\mathrm{s}*}\right) = 0 \end{cases} \tag{24}$$

## V. TRANSFER FUNCTION OF SUSPENSION

The feature parameters of hydropneumatic suspension are defined as follows: mass ratio $\mu = m_2/m_1$, nature frequency of vehicle body $\omega_0 = \sqrt{k/m_2}$, equivalent damping ratio $\xi_{\mathrm{e}} = \lambda/(2m_2\omega_0)$, nature frequency of tire $\omega_{\mathrm{t}} = \sqrt{k_{\mathrm{t}}/m_1}$, and frequency ratio $\gamma = \omega_0/\omega_{\mathrm{t}}$. Considering that the excitation of road roughness is approximately a stationary stochastic process, the statistical transfer function of the hydropneumatic suspension system subjected to the random road disturbance in terms of the power spectrum density can be obtained according to Eq. (24)

$$\begin{cases} H_{z_{1*}}(S) = \dfrac{Z_{1*}(S)}{Z_{\mathrm{r}*}(S)} \\ \qquad\quad = \dfrac{S^4 + 2\gamma\xi_{\mathrm{e}}\omega_{\mathrm{t}}(1+\mu)S^3 + \gamma^2\omega_{\mathrm{t}}^2(1+\mu)S^2}{D(S)} \\ H_{z_{\mathrm{u}*}}(S) = 1 - H_{z_{1*}}(S) = \dfrac{\omega_{\mathrm{t}}^2\left(S^2 + 2\gamma\xi_{\mathrm{e}}\omega_{\mathrm{t}}S + \gamma^2\omega_{\mathrm{t}}^2\right)}{D(S)} \\ H_{z_{2*}}(S) = \dfrac{Z_{2*}(S)}{Z_{\mathrm{r}*}(S)} = \dfrac{\omega_{\mathrm{t}}^2 S^2}{D(S)} \\ H_{z_{\mathrm{s}*}}(S) = H_{z_{\mathrm{u}*}}(S) - H_{z_{2*}}(S) = \dfrac{\gamma\omega_{\mathrm{t}}^3(2\xi_{\mathrm{e}}S + \gamma\omega_{\mathrm{t}})}{D(S)} \\ H_{\ddot{z}_{\mathrm{s}*}}(S) = S^2 H_{z_{\mathrm{s}*}}(S) = \dfrac{\gamma\omega_{\mathrm{t}}^3 S^2(2\xi_{\mathrm{e}}S + \gamma\omega_{\mathrm{t}})}{D(S)} \end{cases} \tag{25}$$

where

$$D(S) = S^4 + 2\gamma\xi_{\mathrm{e}}\omega_{\mathrm{t}}(1+\mu)S^3 + \left(1 + \gamma^2 + \mu\gamma^2\right)\omega_{\mathrm{t}}^2 S^2 + 2\gamma\xi_{\mathrm{e}}\omega_{\mathrm{t}}^3 S + \gamma^2\omega_{\mathrm{t}}^4.$$

$H_{z_{1*}}(S)$ and $H_{z_{2*}}(S)$, respectively, represent the transfer function of the tire deflection and suspension deflection. $H_{z_{\mathrm{u}*}}(S)$ is the displacement transfer function of unsprung mass. $H_{z_{\mathrm{s}*}}(S)$ and $H_{\ddot{z}_{\mathrm{s}*}}(S)$ are the displacement and acceleration transfer functions of sprung mass.

At the same time, the transfer function of the tire relative dynamic load to road excitation can be expressed as:

$$H_{\mathrm{P/G}} = \frac{P/G}{Z_{\mathrm{r}*}} = \frac{k_{\mathrm{t}}(z_{\mathrm{r}*} - z_{\mathrm{u}*})/(m_1+m_2)g}{Z_{\mathrm{r}*}} = \frac{\omega_{\mathrm{t}}^2 H_{z_1}}{(1+\mu)g} \tag{26}$$

Substituting $S = \mathrm{j}\omega$ into the transfer functions, the frequency characteristics of the equivalent linear system under the road surface roughness excitation can be derived.

Typically, the nonlinear algebraic equations can be obtained in the forms of the response of second-order moments and its time derivatives by use of the spectral density approach [15]. A series of standards has been presented by ISO (ISO 1982) for classifying the road roughness based on the power-spectral-density (PSD) results. The PSD of road roughness is simplified as:

$$S_{\mathrm{q}}(n) = G_{\mathrm{q}(n_0)}\left(\frac{n}{n_0}\right)^{-W} \tag{27}$$

where $n$ represents the space frequency ($\mathrm{m}^{-1}$); $n_0$ represents the reference space frequency, and $n_0 = 0.01\ \mathrm{m}^{-1}$; $G_{\mathrm{q}}(n_0)$ denotes the road roughness coefficient, $G_{\mathrm{q}}(\mathrm{n_0}) = 256\mathrm{e}\text{-}6$; and $w$ denotes frequency index which reflects the frequency feature of the pavement, and $w = 2$.

Then, considering the velocity, the excitations of road roughness are obtained in the time and frequency domains:

$$\begin{cases} S_{\mathrm{q}}(f) = \dfrac{1}{v}G_{\mathrm{q}(n_0)}\left(\dfrac{n}{n_0}\right)^{-2} = G_{\mathrm{q}(n_0)}n_0^2\dfrac{v}{f^2} \\ S_{\mathrm{q}}(\omega) = \dfrac{1}{2\pi}S_{\mathrm{q}}(f) = \dfrac{2\pi G_{\mathrm{q}(n_0)}n_0^2 v}{\omega^2} = \dfrac{S_0}{\omega^2} \end{cases} \tag{28}$$

where $v$ denotes the vehicle speed, m/s;$f$ is time frequency, Hz; and $\omega$ is the angular frequency, rad/s; $S_0$ is defined as the road roughness coefficient:

$$S_0 = 2\pi G_{\mathrm{q}(n_0)}n_0^2 v \tag{29}$$

Choosing the power density spectrum of road roughness as input [26]–[28], the acceleration responses of the sprung mass, the velocity responses of the sprung mass, the suspension deflection, and the tire relative dynamic load can be

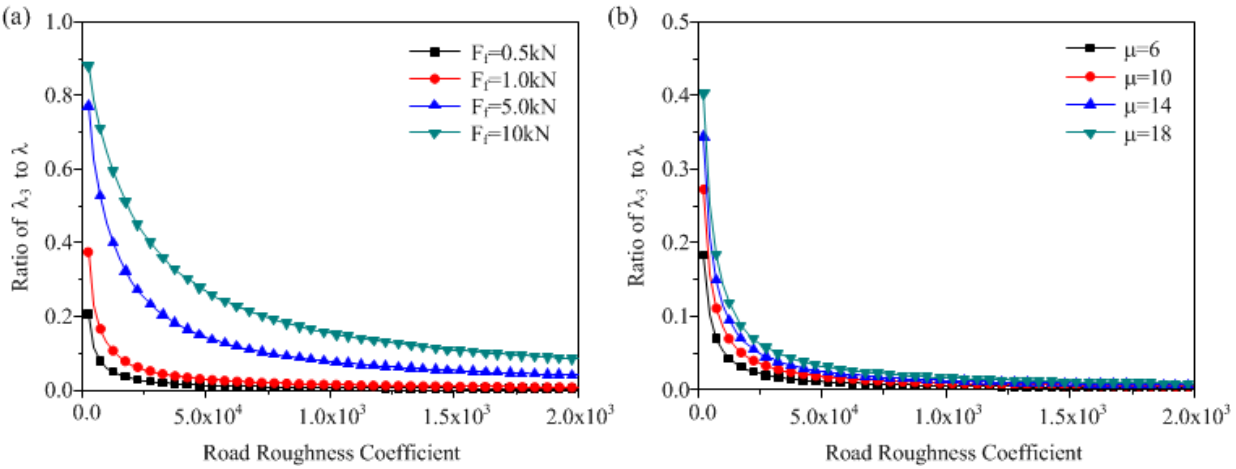


**FIGURE 8.** The ratio of friction damping coefficient to total damping coefficient varying with road roughness coefficient: (a) the damping ratio at different friction force, (b) the damping ratio at different vehicle load.

obtained as follows:

$$\begin{cases} S_{\ddot{z}_{s*}}(\omega) = \left|H_{\ddot{z}_{s*}}(\mathrm{j}\omega)\right|^2 S_q(\omega) = \left|H_{\ddot{z}_{s*}}(\mathrm{j}\omega)\right|^2 \dfrac{S_0}{\omega^2} \\ S_{\dot{z}_{2*}}(\omega) = \left|\mathrm{j}\omega H_{z_{2*}}(\mathrm{j}\omega)\right|^2 S_q(\omega) = \left|H_{z_{2*}}(\mathrm{j}\omega)\right|^2 S_0 \\ S_{z_{2*}}(\omega) = \left|H_{z_{2*}}(\mathrm{j}\omega)\right|^2 S_q(\omega) = \left|H_{z_{2*}}(\mathrm{j}\omega)\right|^2 \dfrac{S_0}{\omega^2} \\ S_{\mathrm{P/G}}(\omega) = \left|H_{\mathrm{P/G}}(\mathrm{j}\omega)\right|^2 S_q(\omega) = \left|H_{\mathrm{P/G}}(\mathrm{j}\omega)\right|^2 \dfrac{S_0}{\omega^2} \end{cases} \tag{30}$$

Using the James Formula [29]–[31], the mean-square values of the vibration acceleration of the hydropneumatic suspension, the vibration velocity of the hydropneumatic suspension and the suspension deflection as well as the tire relative dynamic load are further obtained:

$$\begin{cases} \sigma_{\ddot{z}_s}^2 = \sigma_{\ddot{z}_{s*}}^2 = \displaystyle\int_{-\infty}^{\infty} \left|H_{\ddot{z}_{s*}}(\mathrm{j}\omega)\right|^2 \frac{S_0}{\omega^2}\mathrm{d}\omega \\ = \pi S_0 \omega_t^3 \left[\dfrac{2\gamma\xi_e}{\mu} + \left(1+\dfrac{1}{\mu}\right)\dfrac{\gamma^3}{2\xi_e}\right] \\ \sigma_{z_2}^2 = \sigma_{z_{2*}}^2 = \displaystyle\int_{-\infty}^{\infty} \left|H_{z_{2*}}(\mathrm{j}\omega)\right|^2 S_0 \mathrm{d}\omega = \dfrac{\pi S_0 \omega_t}{2\mu\xi_e\gamma} = \dfrac{\pi S_0 k_t}{\lambda} \\ \sigma_{z_2}^2 = \sigma_{z_{2*}}^2 = \displaystyle\int_{-\infty}^{\infty} \left|H_{z_{2*}}(\mathrm{j}\omega)\right|^2 \frac{S_0}{\omega^2}\mathrm{d}\omega = \dfrac{\pi S_0 (1+\mu)}{2\mu\gamma\xi_e\omega_t} \\ = \dfrac{\pi S_0 (m_1+m_2)}{\lambda} \\ \sigma_{\mathrm{P/G}}^2 = \displaystyle\int_{-\infty}^{+\infty} \left|H_{\mathrm{P/G}}(\mathrm{j}\omega)\right|^2 \frac{S_0}{\omega^2}\mathrm{d}\omega \\ = \dfrac{2\pi S_0 \omega_t^3}{\mu g^2 \xi_e}\left[\dfrac{1}{2\gamma\xi_e(1+\mu)^2} + \dfrac{\gamma^3(1+\mu)}{2\xi_e} \right. \\ \left. - \dfrac{\gamma}{\xi_e(1+\mu)} + 2\gamma\xi_e\right] \end{cases} \tag{31}$$

## VI. PARAMETER DETERMINATION

Based on the results derived above, the linear equivalent coefficients can be further determined and analyzed. Substituting $\sigma_{\dot{z}_2}$ into Eq. (8) and Eq. (15), the following equivalent linear damping coefficients can be yielded.

$$\begin{cases} \lambda_2 = 2R\sqrt{\dfrac{S_0\omega_t}{\mu\xi_e\gamma}} \\ \lambda_3 = 0.798F_f 2R\sqrt{\dfrac{\mu\xi_e\gamma}{S_0\omega_t}} \end{cases} \tag{32}$$

Assuming the parameter values as follows: $R = 1.7 \times 10^5\mathrm{N} \times \mathrm{s}^2\mathrm{m}^2$, $\gamma = 0.2$, $\xi_e = 0.3$, $\omega_t = 60\mathrm{rad/s}$, the ratio of the equivalent friction damping coefficient ($\lambda_3$) to the total damping coefficient ($\lambda$) varying with the road roughness coefficient ($S_0$) is as shown in **Figure 8**. Under the conditions of lower road roughness coefficient, the friction damping is dominant. However, the influences of friction damping on the vehicle system would decrease with the increase of the road roughness coefficient. By contrast, the vehicle load has little impact on the friction damping coefficient. Generally, the friction damping would increase with the increases of friction force. If the friction force $F_f \leq 1\mathrm{kN}$ and the road roughness coefficient $S_0 \geq 1.0 \times 10^3\mathrm{m}^3 \times \mathrm{m\,s}^{-1}$, the influence of friction damping on the vehicle performance is very slight, and it can be neglected.

Equation (22) shows that the vibration responses ($z_u$) of unsprung mass to zero-mean stationary random excitation also follows zero-mean stationary random processes. However, the vibration responses of sprung mass ($z_s$) are nonzero owing to the influence of the hydropneumatic suspension. That is, the suspension is normally at expansion state, i.e., $m_{z_2} \leq 0$, which indicates that the suspension is more likely to generate collision and breakdown at expansion processes. Neglecting the friction damping coefficient and considering Eq. (8) and Eq. VI, the following results can be derived:

$$\begin{cases} \lambda = \sqrt[3]{8R^2 k_t S_0} \\ k = \sqrt{k_1^2 - \frac{4k_2^2\pi(m_1+m_2)S_0}{\lambda}} \end{cases} \tag{33}$$

The parameter values are chosen as follows: $\gamma = 0.2$, $\xi_e = 0.3$, $\omega_t = 60\mathrm{rad/s}$, $m_1 = 650\mathrm{kg}$ $A = 0.0123\mathrm{m}^2$,

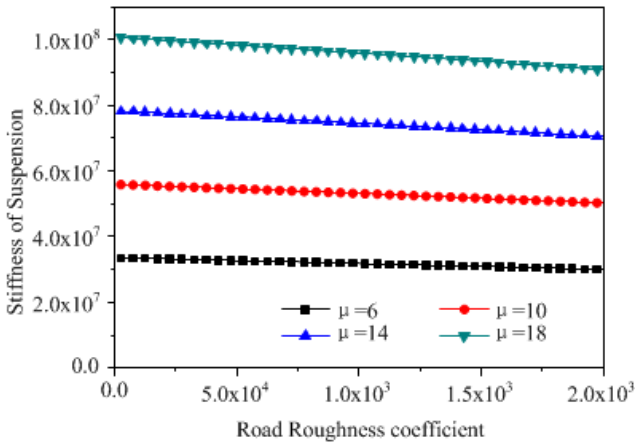


**FIGURE 9.** The relationship between suspension stiffness and road roughness coefficient.

and $V_0 = 0.002\text{m}^3$. Then, the relationships between the suspension stiffness and the road roughness coefficient are shown in **Figure 9**. The road roughness coefficient has little influence on the suspension stiffness. However, the stiffness increases with the increase in vehicle load. This variable behavior of hydropneumatic suspension stiffness makes the natural frequency of the vehicle body relatively stable, which is an important merit of the hydropneumatic suspension and could provide better performance.

According to Eq. (33), the equivalent damping ratio and equivalent frequency ratio are the main factors influencing riding comfort, riding safety handing stability, and suspension reliability. The effects of these system parameters on vehicle performance were analyzed through numerical calculation, and the parameter values are chosen as listed in **Table 1**.

**TABLE 1.** Parameter values for vehicle system.

| Item | $\gamma$ | $\xi_e$ | $\mu$ | $\omega_t$ (rad/s) | $v$ (km/h) |
|---|---|---|---|---|---|
| 1 | 0.1 | 0.1 | 6 | 60 | 25 |
| 2 | 0.2 | 0.2 | 10 | 60 | 40 |
| 3 | 0.3 | 0.3 | 14 | 60 | 55 |
| 4 | 0.4 | 0.4 | 18 | 60 | 70 |

**Figure 10** shows the relationship between tire relative dynamic load and damping ratio. There would be a minimum tire relative dynamic load value when the damping ratio ($\xi_e$) varies in the interval [0.3, 0.5]. Additionally, the tire relative dynamic load is higher if the damping ratio is below 0.2. Under the same damping ratio conditions, the tire relative dynamic load would reduce with reduction in the frequency ratio or increase in the vehicle load.

The relationship between tire relative dynamic load and frequency ratio are depicted in **Figure 11**. When the frequency ratio ($\gamma$) is in the interval [0.1, 0.2], the tire relative dynamic load would have a minimum value. Under the same frequency ratio conditions, the tire relative dynamitic load would reduce with the increase of the damping ratio. The vehicle load has little impact on the tire relative dynamic load because of the variable characteristic of the hydropneumatic suspension stiffness.

As shown in **Figure 12**, the acceleration of vehicle body would have a minimum value when the damping ratio ($\gamma$) is in the interval [0.2, 0.3]. The acceleration of vehicle body would increase rapidly if the damping ratio is below 0.2. Under the same damping ratio conditions, the acceleration of vehicle body would reduce with reduction in the frequency ratio or increase in the vehicle load.

The acceleration of vehicle body would increase approximately linearly with the increase of the frequency ratio, as shown in **Figure 13**. Under the same frequency ratio conditions, it would decrease with the reduction of damping ratio. The vehicle load has little impact on the acceleration of the vehicle body because the hydropneumatic suspension possesses variable stiffness characteristics.

The suspension deflection is higher when the damping ratio is below 0.2, which indicates that a small damping ratio would be cause suspension breakdown very easily, as shown in **Figure 14**. Under the same damping ratio conditions, the suspension deflection would increase with the reduction of the frequency ratio. By contrast, the stiffness would increase with the vehicle load, so the deflection would stay relatively stable at different vehicle load conditions. The vehicle load would have little impact on the suspension deflection.

The suspension deflection would reduce with the increase of frequency ratio, as shown in **Figure 15**. If the frequency ratio is below 0.2, the suspension deflection is higher. The suspension can have a breakdown very easily when a small frequency ratio is designed. Consequently, the natural frequency of the vehicle body cannot be reduced without limitation. Comprehensively, the following design principles are obtained through analyzing the numerical calculation results:

The tire dynamic load would have a minimum value when the equivalent damping ratio ($\gamma$) is in the interval [0.3, 0.5]. However, there would be a minimum vehicle body acceleration if the equivalent damping ratio ($\xi_e$) is in the interval [0.2, 0.3]. When the damping ratio is below 0.2, the tire relative dynamitic load, vehicle body acceleration and suspension deflection are relatively higher. Consequently, it is reasonable to choose a damping ratio above 0.2 but no more than 0.5.

The vehicle body acceleration and the tire relative dynamic load would linearly increase with the increase in the frequency ratio. In addition, there would be a minimum tire relative dynamic load when the frequency ratio is in the interval [0.1, 0.2]. These conclusions indicate that a lower frequency ratio is beneficial for reducing the vehicle body acceleration and improving riding comfort. However, the suspension deflection is much higher and easily leads

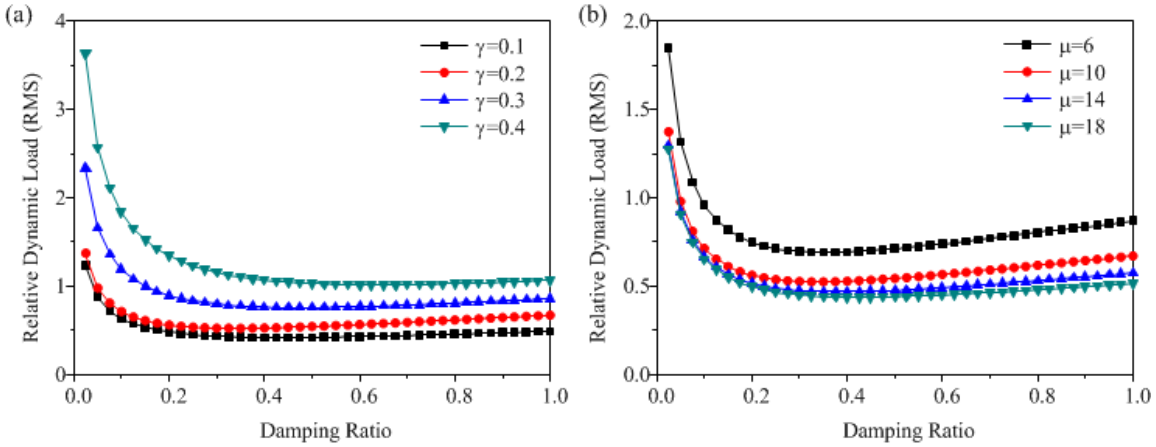


**FIGURE 10.** The relationship between tire relative dynamic load and damping ratio: (a) the relative dynamic load at different frequency ratio, (b) the relative dynamic load at different vehicle load.

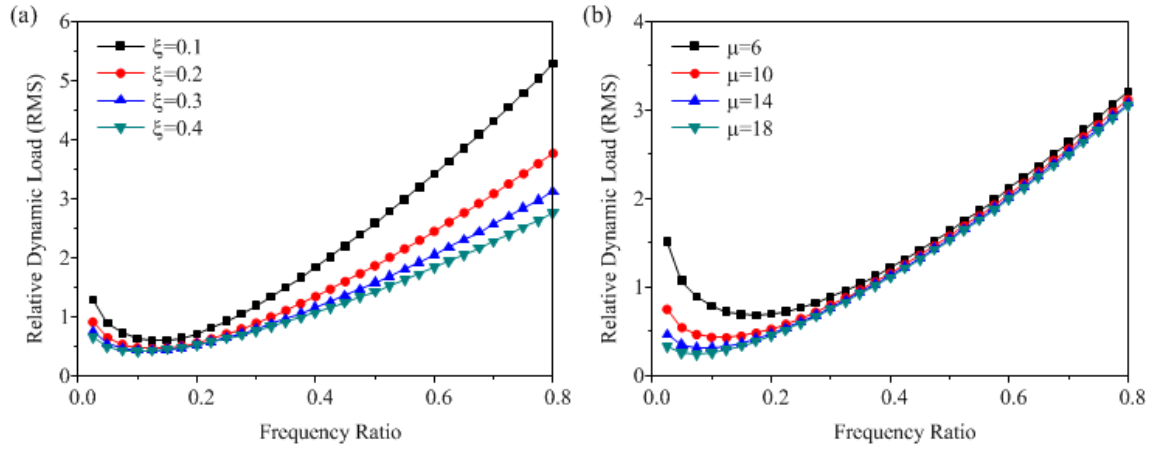


**FIGURE 11.** The relationship between tire relative dynamic load and frequency ratio: (a) the relative dynamic load at different damping ratio, (b) the relative dynamic load at different vehicle load.

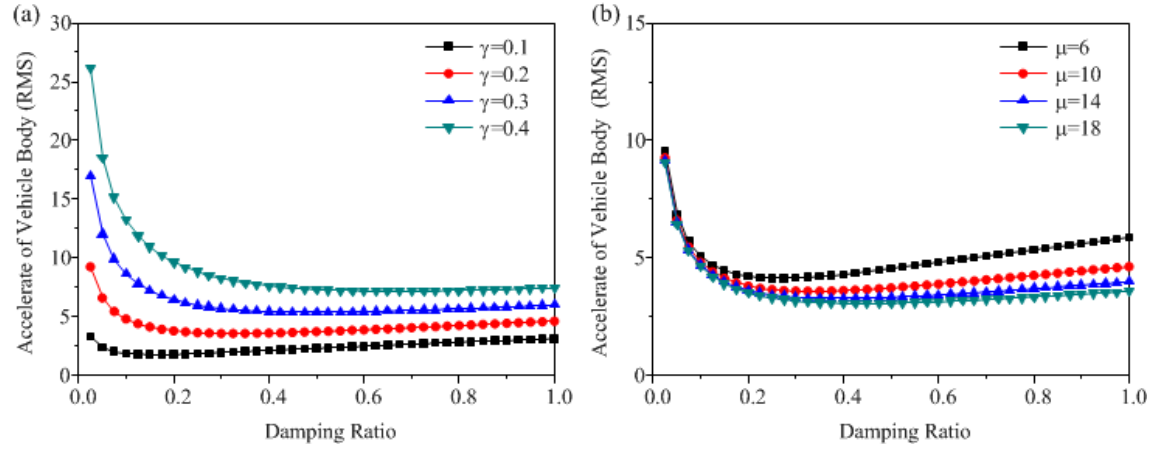


**FIGURE 12.** The relationship between the vehicle body acceleration and damping ratio: (a) the vehicle body acceleration at different frequency ratio, (b) the vehicle body acceleration at different vehicle load.

to suspension breakdown if the frequency ratio is below 0.2; the suspension reliability would dramatically worsen. Therefore, the frequency ratio should be chosen to maintain balance suspension reliability and riding comfort.

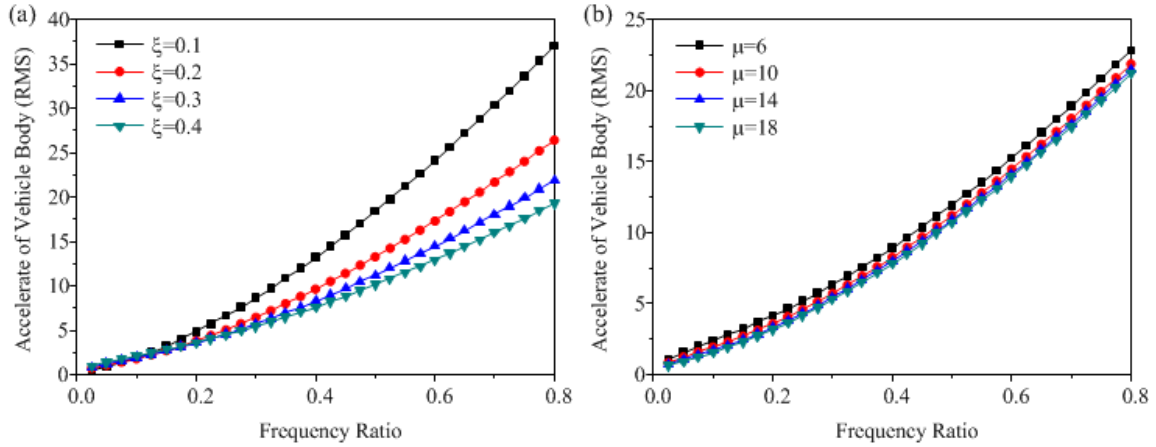


**FIGURE 13.** The relationship between the acceleration of vehicle body and frequency ratio: (a) the acceleration of vehicle body at different damping ratio, (b) the acceleration of vehicle body at different vehicle load.

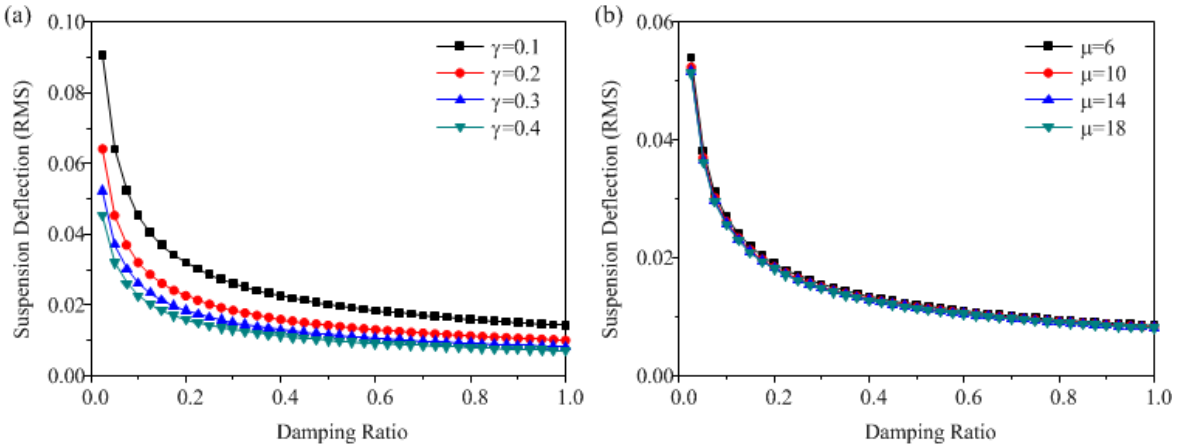


**FIGURE 14.** The relationship between suspension deflection and damping ratio: (a) the suspension deflection at different frequency ratio, (b) the suspension deflection at different vehicle load.

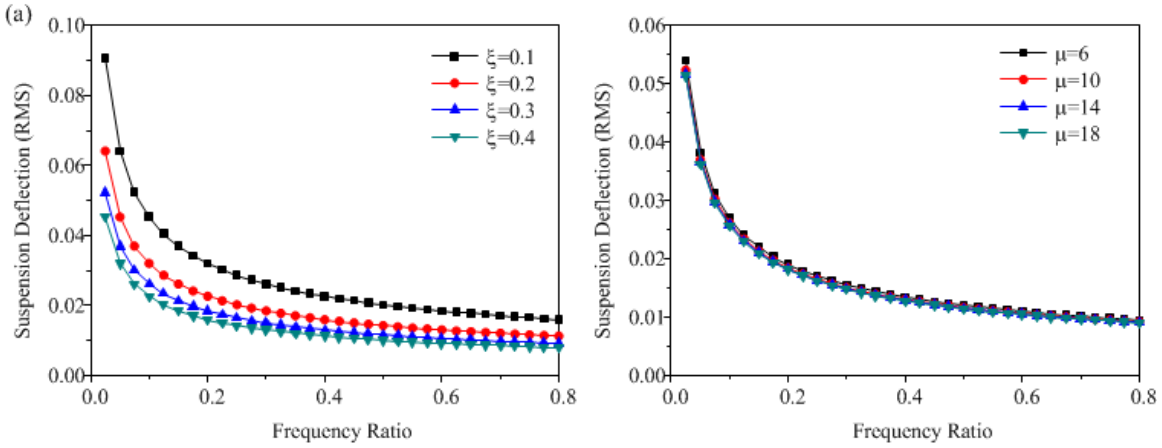


**FIGURE 15.** The relationship between suspension deflection and frequency ratio: (a) the suspension deflection at different damping ratio, (b) the suspension deflection at different vehicle load.

When the vehicle load increases moderately, i.e., the mass ratio increases in a reasonable range, the vehicle body acceleration reduces and the riding comfort is improved. Meanwhile, the handing stability and the suspension reliability are also accordingly improved.

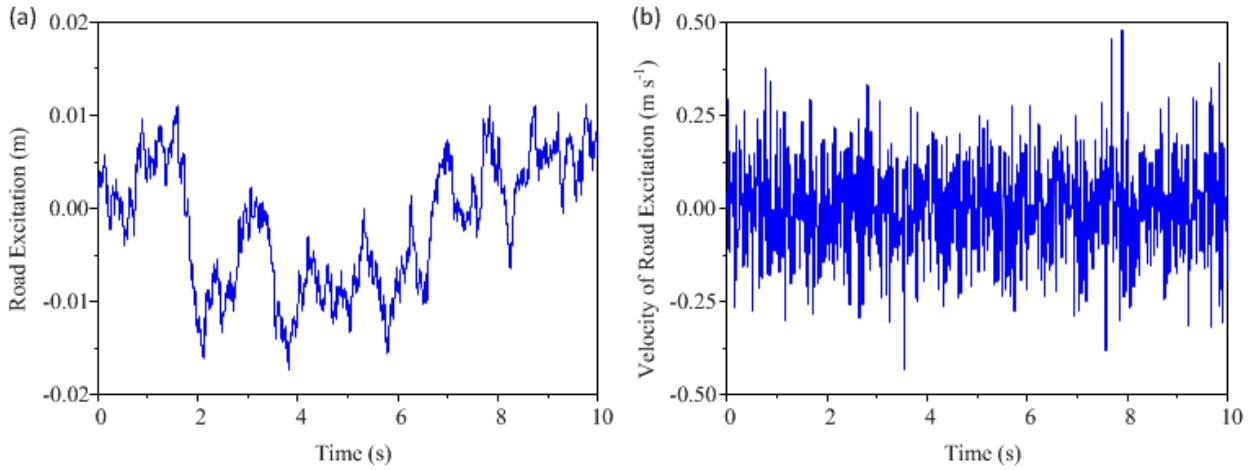


**FIGURE 16.** The displacement and velocity of road excitation: (a) the displacement of road excitation, (b) the velocity of road excitation.

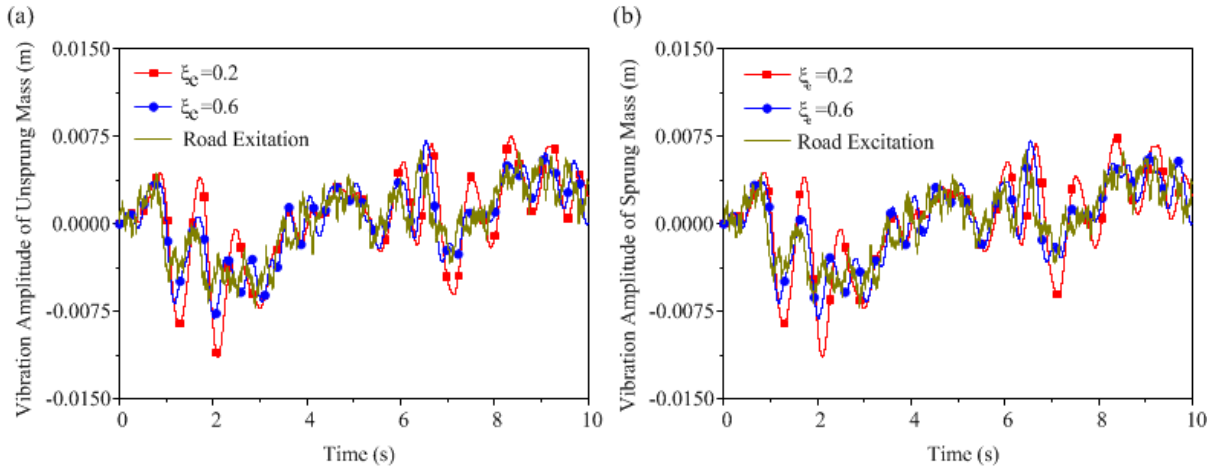


**FIGURE 17.** The vibration of sprung mass and unsprung mass excited by road roughness: (a) vibration of sprung mass, (b) the vibration of unsprung mass.

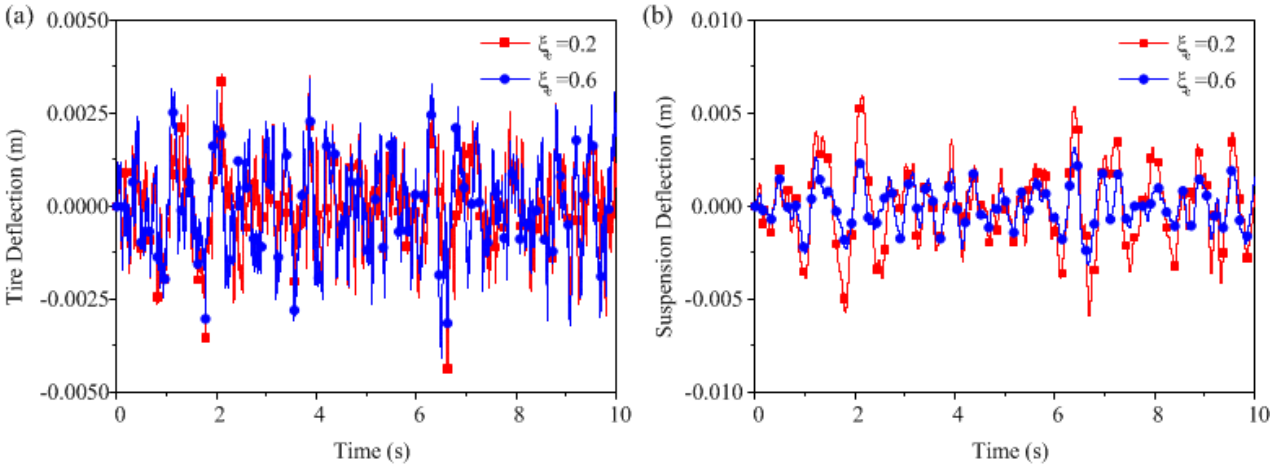


**FIGURE 18.** The tire deflection and suspension deflection excited by road roughness: (a) the tire deflection, (b) the suspension deflection.

## VII. SIMULATION AND DISCUSSION

In this section, the performances of hydropneumatic suspension system subjected to random road surface are simulated. The parameters are chosen based on the analysis in the previous section, and the parameters for simulation are listed in **Table 2**.

**TABLE 2.** The parameter values for hydropneumatic suspension system.

| Item | Variable | Specification | unit |
|---|---|---|---|
| Sprung mass | $m_1$ | 3250 | kg |
| Unsprung mass | $m_2$ | 650 | kg |
| Velocity | $v$ | 20 | m $s^{-1}$ |
| Piston area | $A$ | 0.0123 | $m^2$ |
| Gas chamber volume | $V_0$ | 0.002 | $m^3$ |
| Gas chamber pressure | $p_0$ | 5 | MPa |
| Oil density | $\rho$ | 880 | kg $m^{-3}$ |
| Tire stiffness | $k_t$ | 7.8×105 | N $m^{-1}$ |

Utilizing the integrated Gaussian white noise, the model for random road excitation is built in the time domain as follows:

$$\dot{S}_q(\omega) = n_0\sqrt{2\pi G_{q(n_0)}v}W(t) - 2\pi n_{00}vS_q(\omega) \qquad (34)$$

where $W(t)$ denotes the Gaussian white noise, $n_{00}$ denotes the low cut-off space frequency (here, $n_{00} = 0.011$ $m^{-1}$), and $v$ denotes the vehicle speed (here, $v = 20$ m $s^{-1}$).

Under specific riding conditions (C class road, and $v = 20$ m $s^{-1}$), the irregular road profiles and the velocity of road excitation are obtained based on Eq. (34). As shown in **Figure 16**, the maximum vibration amplitude is approximately 18 mm in the time domain, and the maximum vibration velocity is approximately 0.5 m $s^{-1}$.

At the specified riding conditions mentioned above, the vibrations of unsprung mass and sprung mass with respect to random road excitation are shown in **Figure 17**. The unsprung mass and sprung mass have the same movement trend with road profile, which indicates that the tire can grasp the road well and has good handing stability. The vibration amplitudes are slightly higher than those of the road profile, but the high frequency components are eliminated by the suspension system. The elimination of high frequency vibration is of benefit to improving the riding comfort.

The tire deflection and suspension deflection excited by road roughness are shown in **Figure 18**. The suspension deflection is slightly higher than the tire deflection, and the suspension has lower deflection frequency. This means that the advantages of the tire and suspension are fully used and that the vehicle has good riding comfort. Damping ratio is an important effect factor on the property of hydropneumatic suspension system. The lower damping ratio would reduce the tire deflection amplitude and frequency. Simultaneously, the lower damping ratio would enlarge the suspension deflection amplitude and reduce the suspension deflection frequency. In other words, the lower damping ratio is of benefit to improving riding comfort, but it also increases the risk of suspension break. Consequently, the damping ratio should be designed suitably considering the riding comfort and suspension reliability.

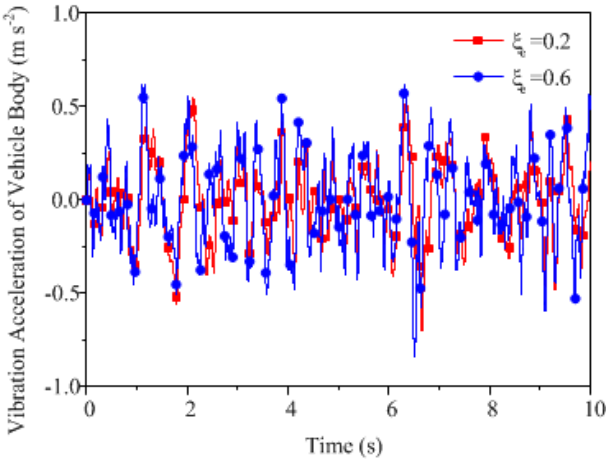


**FIGURE 19.** The vibration acceleration of vehicle body excited by road roughness.

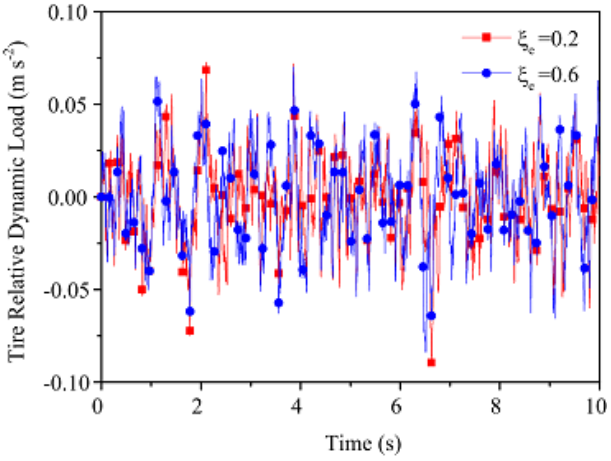


**FIGURE 20.** The relative dynamic load of tire excited by road roughness.

The vibration acceleration of the vehicle body is another important parameter to determine the riding comfort performance. The lower acceleration means better riding comfort quality. As shown in **Figure 19**, the maximum vibration acceleration is approximately 0.7 $ms^{-2}$ at the damping ratio of 0.6, and the vibration acceleration is lower at the damping ratio of 0.2, which means that the hydropneumatic suspension system has a better performance on vibration suppression at lower damping ratio conditions.

The tire relative dynamic load is associated with riding safety, and a lower value is considered better. The simulation results agreed well with the numerical calculations in the previous section. As shown in **Figure 20**, the tire relative dynamic load is higher at a damping ratio of 0.2 than at the damping of 0.6, which is detrimental to the riding comfort. In other words, it is hard to achieve the best riding comfort and the best riding safety at the same time. Consequently, a suitable damping ratio should be chosen to maintain the

balance between riding comfort and riding safety. In general, it is better to determine the damping ratio at the intervals [0.2, 0.5].

## VIII. CONCLUSION

This study designed a hydropneumatic spring and proposed the theoretical principle for parameter determination. A quarter-vehicle model with the characteristics of nonlinear stiffness, nonlinear hydraulic damping and nonlinear friction damping was built. The nonlinear mathematical model was linearized by use of the statistical linearization method on the basis of random vibration theory. Furthermore, the transfer functions of the tire relative dynamic load, the vehicle body acceleration and the suspension deflection subjected to the road roughness excitation were obtained, and the responses to the wide band random road roughness excitation were analyzed according to the James Formula. The influences of the equivalent damping ratio and equivalent frequency ratio on the vehicle riding comfort and handing stability were analyzed. These analyses indicated that a larger damping ratio was beneficial for reducing the tire relative dynamitic load in the interval [0.3, 0.5], and it is also better for vehicle body acceleration in the interval [0.2, 0.3]. Consequently, the damping ratio was generally designed to be approximately 0.3 to maintain a balance between riding comfort and riding safety. The vehicle body acceleration and tire relative dynamic load would tend to decreased linearly with the reduction of the frequency ratio. However, the frequency ratio was generally set not less than 0.2 owing to the limitation of the suspension deflection. A relatively higher vehicle load was helpful for maintaining the riding comfort, the handing stability and the vehicle safety.

## REFERENCES

[1] F. Beltrán-Carbajal, E. Chávez-Conde, A. Favela-Contreras, and R. Chávez-Bracamontes "Active nonlinear vehicle suspension control based on real-time estimation of perturbation signals," in *Proc. IEEE Int. Conf. Ind. Technol. (ICIT)*, Auburn, AL, USA, Mar. 2011, pp. 437–442.
[2] J. Marzbanrad, G. Ahmadi, H. Zohoor, and Y. Hojjat, "Stochastic optimal preview control of a vehicle suspension," *J. Sound Vib.*, vol. 275, nos. 3–5, pp. 973–990, Aug. 2004.
[3] Y. Jin and X. Luo, "Stochastic optimal active control of a half-car nonlinear suspension under random road excitation," *Nonlinear Dyn.*, vol. 72, nos. 1–2, pp. 185–195, Apr. 2013.
[4] U. Solomon and C. Padmanabhan, "Hydro-gas suspension system for a tracked vehicle: Modeling and analysis," *J. Terramechanics*, vol. 48, no. 2, pp. 125–137, Apr. 2011.
[5] H. Ren, S. Chen, Y. Zhao, G. Liu, and L. Yang, "State observer-based sliding mode control for semi-active hydro-pneumatic suspension," *Vehicle Syst. Dyn.*, vol. 54, no. 2, pp. 168–190, 2016.
[6] M. D. Emami, S. A. Mostafavi, and P. Asadollahzadeh, "Modeling and simulation of active hydro-pneumatic suspension system through bond graph," *Mechanics*, vol. 17, no. 3, pp. 312–317, 2011.
[7] S.-A. Chen, J.-C. Wang, M. Yao, and Y. -B. Kim, "Improved optimal sliding mode control for a non-linear vehicle active suspension system," *J. Sound Vib.*, vol. 395, pp. 1–25, May 2017.
[8] L. Xiao and Y. Zhu, "Sliding-mode output feedback control for active suspension with nonlinear actuator dynamics," *J. Vib. Control*, vol. 21, no. 14, pp. 2721–2738, Oct. 2015.
[9] S. Narayanan and S. Senthil, "Stochastic optimal active control of a 2-DOF quarter car model with non-linear passive suspension elements," *J. Sound Vib.*, vol. 211, no. 3, pp. 495–506, Apr. 1998.
[10] S. Narayanan and G. V. Raju, "Active control of non-stationary response of vehicles with nonlinear suspensions," *Vehicles Syst. Dyn.*, vol. 21, no. 1, pp. 73–87, 1992.
[11] Y. K. Wen, "Equivalent linearization for hysteretic systems under random excitation," *J. Appl. Mech.*, vol. 47, pp. 150–154, Mar. 1980.
[12] G. Verros, S. Natsiavas, and C. Papadimitriou, "Design optimization of quarter-car models with passive and semi-active suspensions under random road excitation," *J. Vib. Control*, vol. 11, pp. 581–606, May 2005.
[13] C. J. Dodds and J. D. Robson, "The description of road surface roughness," *J. Sound Vib.*, vol. 31, no. 2, pp. 175–183, Mar. 1973.
[14] K. M. A. Kamash and J. D. Robson, "Implications of isotropy in random surfaces," *J. Sound Vib.*, vol. 54, no. 1, pp. 131–145, Oct. 1977.
[15] T. S. Atalik and S. Utku, "Stochastic linearization of multi-degree-of-freedom non-linear systems," *Earthquake Eng. Struct. Dyn.*, vol. 4, no. 4, pp. 411–420, Apr. 1976.
[16] A. G. Thompson and B. R. Davis, "Computation of the rms state variables and control forces in a half-car model with preview active suspension using spectral decomposition methods," *J. Sound Vib.*, vol. 285, pp. 571–583, Jul. 2005.
[17] S. Türkay and H. Akçay, "A study of random vibration characteristics of the quarter-car model," *J. Sound Vib.*, vol. 282, pp. 111–124, Apr. 2005.
[18] S. Q. Wu and S. S. Law, "Vehicle axle load identification on bridge deck with irregular road surface profile," *Eng. Struct.*, vol. 33, pp. 591–601, Feb. 2011.
[19] M. Dong and Z. Luo, "Statistical linearization on 2 DOFs hydropneumatic suspension with asymmetric non-linear stiffness," *Chin. J. Mech. Eng.*, vol. 28, no. 3, pp. 504–510, May 2015.
[20] W. D. Iwan and I.-M. Yang, "Application of statistical linearization techniques to nonlinear multidegree-of-freedom systems," *J. Appl. Mech.*, vol. 39, no. 2, pp. 545–550, Jun. 1972.
[21] W. D. Iwan, "A generalization of the concept of equivalent linearization," *Int. J. Non-Linear Mech.*, vol. 8, no. 3, pp. 279–287, Jun. 1973.
[22] T. K. Caughey, "Equivalent linearization techniques," *J. Acoust. Soc. Amer.*, vol. 35, no. 11, pp. 1706–1711, 1963.
[23] L. V. V. G. Rao and S. Narayanan, "Preview control of random response of a half-car vehicle model traversing rough road," *J. Sound Vib.*, vol. 310, pp. 352–365, Feb. 2008.
[24] L. V. V. G. Rao and S. Narayanan, "Sky-hook control of nonlinear quarter car model traversing rough road matching performance of LQR control," *J. Sound Vib.*, vol. 323, pp. 515–529, Jun. 2009.
[25] U. Von Wagner, "On non-linear stochastic dynamics of quarter car models," *Int. J. Non-Linear Mech.* vol. 39, pp. 753–765, Jul. 2004.
[26] K. Bogsjö, K. Podgórski, and I. Rychlik, "Models for road surface roughness," *Vehicle Syst. Dyn.*, vol. 50, no. 5, pp. 725–747, 2012.
[27] L.-X. Guo and L.-P. Zhang, "Robust $H_\infty$ control of active vehicle suspension under non-stationary running," *J. Sound Vib.*, vol. 331, no. 26, pp. 5824–5837, Dec. 2012.
[28] *Mechanical Vibration—Road Surface Profiles—Reporting Of Measured Data*, document ISO 8608, 1995(E), International Organization for Standardization, ISO, 1995.
[29] D. E. Newland, *An Introduction to Random Vibrations and Spectral Analysis*. Chelmsford, MA, USA: Courier, 2012.
[30] H. M. James, N. B. Nichols, and R. S. Phillips, *Theory of Servomechanisms*. New York, NY, USA: McGraw Hill, 1947.
[31] S. H. Crandall and W. D. Mark, *Random Vibration in Mechanical Systems*. New York, NY, USA: Academic, 1963.

**ZUTI ZHANG** received the B.S. degree in mechanical engineering from Northwest A&F University, Xi'an, China, in 2010, and the Ph.D. degree in mechanical engineering from the Huazhong University of Science and Technology, Wuhan, China, in 2017. He is currently a Post-Doctoral Researcher with the School of Naval Architecture and Ocean Engineering, Huazhong University of Science and Technology. His current research interests include water hydraulics components and system, high-pressure waterjet propulsion technology, marine mechatronic systems, electro-hydraulic control, and hydro-pneumatic suspension.

**SHUPING CAO** received the B.S., M.S., and Ph.D. degrees in mechanical engineering from the Huazhong University of Science and Technology, Wuhan, China, in 1988, 1991, and 2002, respectively. Then, he joined the School of the Mechanical Science and Engineering, Huazhong University of Science and Technology, as an Assistant Teacher, where he has been an Assistant Professor since 2000. His research interests include hydraulic-pneumatic suspension system, electro-hydraulic control system, and ships operation and control system.

**CHUNHONG RUAN** received the B.S. degree in mechanical engineering from the Huazhong University of Technology, Wuhan, China, in 1988. In 1996, she joined the School of the Mechanical Science and Engineering, Huazhong University of Science and Technology, where she has been an Assistant Professor since 2001. She has authored more than 10 books. Her research interests include hydraulic damping, intelligence and simulation design, and engineering graphics.